

Effect of uniaxial stress on the interference of polaritonic waves in wide quantum wellsD. K. Loginov,¹ A. V. Trifonov,² and I. V. Ignatiev²¹*St. Petersburg State University, St. Petersburg 198504, Russia*²*Spin Optics Laboratory, St. Petersburg State University, St. Petersburg 198504, Russia*

(Received 24 April 2014; revised manuscript received 23 July 2014; published 12 August 2014)

A theory of polaritonic states is developed for a nanostructure with a wide quantum well stressed perpendicular to the growth axis of the heterostructure. The role of the \mathbf{K} -linear terms appearing in the exciton Hamiltonian under the stress is discussed. Exciton reflectance spectra are theoretically modeled for the nanostructure. It is predicted that the spectral oscillations caused by interference of the excitonlike and photonlike polariton modes disappear with the increase of applied pressure and then appear again with the opposite phase relative to that observed at low pressure. Effects of gyrotropy and convergence of masses of excitons with heavy and light holes due to their mixing by the deformation are also considered. Numerical estimates performed for the GaAs wells show that these effects can be experimentally observed at pressure $P < 1$ GPa for the well widths of a fraction of a micron.

DOI: [10.1103/PhysRevB.90.075306](https://doi.org/10.1103/PhysRevB.90.075306)

PACS number(s): 71.35.-y, 71.36.+c, 71.70.Fk, 78.67.De

I. INTRODUCTION

Carrier motion in direct-gap semiconductors is usually described by a parabolic dispersion law that is by quadratic dependence of energy on wave vector \mathbf{K} . In many cases, however, \mathbf{K} -linear terms in the carrier Hamiltonian may play an important role. These terms become important, in particular, when the inversion asymmetry is broken for bulk crystal (bulk inversion asymmetry, BIA) or the asymmetry of the heteropotential, e.g., in quantum wells (QWs) and superlattices, is present (structure inversion asymmetry, SIA). Both the BIA and SIA give rise to the \mathbf{K} -linear splittings of carrier states with opposite spins [1–4]. These splittings manifest themselves in such effects as spin orientation and relaxation [5], weak antilocalization (WAL) [6–8], circular photogalvanic effect [9], and gyrotropy [10–13].

Recently, a new type of semiconductor structures, in which the carrier energy is linearly dependent on the wave vector, has become actively studied [14,15]. Several unusual effects are observed for such structures. For example, the finite conductivity at low carrier concentrations and an anomalous quantum Hall effect are observed in graphene [16]. Basic physics of topological insulators is also related to \mathbf{K} -linear dispersion of edge states which are, as a rule, protected against disorder (see, e.g., Refs. [15,17]).

When the electron and hole, whose energy depend on \mathbf{K} -linear terms, are combined into an exciton, its Hamiltonian should include the \mathbf{K} -linear terms also. These terms affect such phenomena as ballistic spin transport [18] and vortices [19] in exciton condensates. In wide QWs, excitons with large wave vectors become observable [20,21] and the effects caused by the \mathbf{K} -linear terms should reveal themselves as strongly as possible.

The interaction of excitons with light can be described as polaritonic excitations of crystal. A wide QW is a resonator for polaritons and therefore they become standing waves, which manifest themselves as oscillations in the reflection or absorption spectra [20,21]. Theoretical calculations of reflection spectra for ZnSe/ZnSsSe and GaAs/AlGaAs QWs show reasonable agreement with experimental data in the framework of the simplest model, in which the exciton energy

quadratically depends on the exciton wave vector \mathbf{K} [22,23], although the \mathbf{K} -linear terms should be present in the exciton Hamiltonian at least due to the BIA effect in the QWs. The reason for that is the relatively small effect of \mathbf{K} -linear terms for unstrained heterostructures.

The role of the \mathbf{K} -linear terms can dramatically increase if a uniaxial stress is applied to the structure with the BIA and SIA. The stress results in the \mathbf{K} -linear splitting of the lowest conduction band and the upper valence band (see, e.g., [24]). Although the effect of uniaxial stress has been known for several decades, its possible impact on the exciton and, accordingly, on the polariton spectra of wide QWs has not been investigated yet.

In this paper, we present a theoretical analysis of the interference of polariton waves in a wide QW subject to the uniaxial stress. We discuss the effects induced by the stress applied perpendicular to the direction of the propagation of polariton waves. As will be shown, the stress leads to \mathbf{K} -linear contributions to the energy of the electrons and holes. This results in the modification of polaritonic states in the QW and, as a consequence, in the dramatic change of reflection spectra. In addition, the uniaxial stress leads to intermixing of the heavy-hole and light-hole excitons and to a “convergence” of their effective masses.

Theoretical modeling of polariton spectra is fulfilled for a GaAs/AlGaAs QW. The quality of GaAs-based QWs grown by molecular-beam epitaxy is high enough now to observe effects related to the \mathbf{K} -linear splitting of exciton states. The estimates given below show that the theoretically predicted effects can be observed at pressures available experimentally.

Analysis of the effect of uniaxial stress on the polariton states will be performed in the following sequence. In Sec. II, we consider the Hamiltonian of an exciton in the presence of the uniaxial stress without an interaction with light. Section III is devoted to a description of the permittivity of the strained crystal in the presence of the exciton-light interaction. In addition, calculations of the dispersion relations for the polariton modes are given in this section. In Sec. IV, we define the boundary conditions for the polariton modes. The main results are present in Secs. V and VI. The microscopic nature of the suppression and recovery of oscillations in the polariton

spectra is discussed in Sec. VII. The last section summarizes the main findings and conclusions.

II. HAMILTONIAN OF AN EXCITON IN THE PRESENCE OF STRESS

Consider an exciton in a crystal with the zinc-blende symmetry, propagating along the Z axis, which coincides with the [001] crystallographic axis. Such exciton is characterized by only one nonzero component of the exciton wave vector $K = K_z, K_x = K_y = 0$. In what follows, we consider this direction as the quantization axis for the angular momenta of carriers.

The exciton states observed in the optical experiments in crystals such as GaAs are formed from the states of the doubly degenerate conduction band Γ_6 and the fourfold degenerate valence band Γ_8 . The wave functions of electrons and holes in this approximation are, respectively, two- and four-component plane waves [25].

We derive the excitonic Hamiltonian from the Hamiltonians of free electrons and holes. In what follows, we neglect the terms related to the corrugation of the valence band [25], which are responsible for mixing heavy and light holes. These effects are weak compared to those caused by the terms included in the spherically symmetric part of the valence-band Hamiltonian and do not affect the phenomena discussed in the present paper.

To construct the excitonic Hamiltonian, we replace the coordinates of free electrons, \mathbf{r}_e , and of heavy and light holes, $\mathbf{r}_{hh}, \mathbf{r}_{lh}$, by coordinates of motion of the exciton as a whole, $Z = (z_e m_e + z_{hh, lh} m_{hh, lh}) / (m_e + m_{hh, lh})$, and of the relative motion of the electron and hole, $\mathbf{r} = \mathbf{r}_e - \mathbf{r}_{hh, lh}$. Here, m_e, m_{hh} , and m_{lh} are effective masses of the electron, heavy hole, and light hole, respectively.

The effects considered below are observed in the spectral range where the kinetic energy of the exciton is comparable with its binding energy. Excitons with such kinetic energy can be described in the approximation of the ‘‘large’’ wave vector [26]. According to this approximation, operators of the wave vectors for free electrons and holes can be expressed as follows:

$$\begin{aligned} \hat{k}_x^{(e, hh, lh)} &= \pm \frac{\hat{p}_x}{\hbar}, \quad \hat{k}_y^{(e, h)} = \pm \frac{\hat{p}_y}{\hbar}, \\ \hat{k}_z^{(e, hh, lh)} &= \pm \frac{\hat{p}_z}{\hbar} + \frac{m_{e, hh, lh}}{m_e + m_{hh, lh}} \hat{K}_z, \end{aligned} \quad (1)$$

where the signs ‘‘+’’ and ‘‘-’’ refer to electrons and holes, respectively. Here, $m_{hh, lh} = m_0 / (\gamma_1 \pm \gamma_2)$, where m_0 is a free-electron mass and γ_1, γ_2 are the Luttinger parameters [25]. Operator $\hat{p}_{x(y, z)} = -i\hbar\partial/\partial x(y, z)$ is the momentum operator of relative motion of the electron and hole; $\hat{K}_z = -i\partial/\partial Z$ is the operator of wave vector of the exciton motion as a whole; $M_{h, l} = m_e + m_{hh, lh}$ denote translational masses of the heavy-hole and light-hole excitons. The Hamiltonian of the excitons is

$$\hat{H}_{Xh, l}^{(0)} = \hat{H}_{Kh, l}^{(0)} + \hat{H}_p^{(0)}, \quad (2)$$

where

$$\hat{H}_{Kh, l}^{(0)} = E_g + \frac{\hbar^2 \hat{K}^2}{2M_{h, l}} \quad (3)$$

is the Hamiltonian of the exciton motion as a whole; and

$$\hat{H}_p^{(0)} = \frac{\hat{p}^2}{2\mu} - \frac{e^2}{\epsilon_0 r} \quad (4)$$

is the Hamiltonian of relative motion of the electron and hole. In Eqs. (2)–(4), E_g is a band gap, $\mu = 1/m_e + \gamma_1/m_0$ is a reciprocal exciton mass, ϵ_0 is a background permittivity of the crystal, and e is the electron charge. The coordinate part of the wave function of exciton has the form

$$\Psi(K) = e^{iKZ} F_{NLM}, \quad (5)$$

where F_{NLM} is the hydrogenlike wave function of the relative motion of electron and hole. This function can be represented as $F_{NLM} = \mathcal{R}_{NL} \mathcal{Y}_{LM}$, where \mathcal{R}_{NL} and \mathcal{Y}_{LM} are radial and spherical functions, respectively. Subscript \mathcal{N} is the principal quantum number and subscripts \mathcal{L}, \mathcal{M} are the orbital angular momentum and its projection on the quantization axis, respectively.

The Hamiltonian given by Eq. (2) does not mix orbital states of the exciton. Uniaxial stress can lead to mixing of $1s$ - and p -exciton states; however, this effect can be neglected because of its smallness (see below). Hence we consider only the $1s$ -exciton state with $N = 1, L = 0$, and $M = 0$. The wave function of this state contains the components $\mathcal{R}_{10} = 2e^{-r/a_B}$ and $\mathcal{Y}_{00} = 1/\sqrt{4\pi}$, where $a_B = \epsilon_0 \hbar^2 / \mu e^2$ is the exciton Bohr radius. Note that the coordinate parts of wave functions for the heavy-hole and light-hole excitons are the same up to some constant [27]. The energy of the $1s$ exciton in the unstrained crystal has the form

$$H_{Xh, l}^{(0)} = E_X + \frac{\hbar^2 K^2}{2M_{h, l}}, \quad (6)$$

where $E_X = E_g - R$ is the energy of an optical transition to the exciton ground state, and $R = \mu e^4 / (2\hbar^2 \epsilon_0^2)$ is the exciton binding energy, which is the eigenvalue of the operator given by Eq. (4).

The Hamiltonian of the exciton motion in the unstrained crystal can be written as a matrix 8×8 consisting of two identical blocks 4×4 , which have the form

$$\hat{H}_X^{(0)} = \begin{pmatrix} H_{Xh}^{(0)} & 0 & 0 & 0 \\ 0 & H_{Xl}^{(0)} & 0 & 0 \\ 0 & 0 & H_{Xl}^{(0)} & 0 \\ 0 & 0 & 0 & H_{Xh}^{(0)} \end{pmatrix}. \quad (7)$$

One of these blocks describes the optically active exciton states with spin projections ± 1 , and the second one is the optically inactive states with spin projections ± 2 and 0 for light-hole and heavy-hole excitons, respectively. The matrix of the Hamiltonian (7) is written in the basis of eight-component plane waves, which we denote as

$$|j, s\rangle_K = v_{j, s} \Psi(K). \quad (8)$$

Here, $v_{j, s}$ are the eight-component spinors, in which one component is equal to the unit, and others are zero. $j = \pm 3/2, \pm 1/2$ and $s = \pm 1/2$ are the projections of the spin moment of electron and hole, respectively, and $\Psi(K)$ is given by Eq. (5).

Uniaxial stress leads to two main effects. One of them is a change of the energy structure of the Γ_8 valence band. This

effect is described by the Bir-Pikus Hamiltonian [28]:

$$\hat{H}_\varepsilon = -a\mathbb{I}\text{Sp}(\varepsilon) + b \sum_{\alpha} J_{\alpha}^2 \left[\varepsilon_{\alpha\alpha} - \frac{1}{3}\text{Sp}(\varepsilon) \right] + d \sum_{\alpha \neq \beta} \varepsilon_{\alpha\beta} \{J_{\alpha}, J_{\beta}\}, \quad (9)$$

where \mathbb{I} denotes the unit matrix, $\varepsilon_{\alpha\beta}$ is the strain tensor, and $\text{Sp}(\varepsilon) = \sum_{\alpha} \varepsilon_{\alpha\alpha}$. Matrices J_{α} denote the hole angular momentum, where $\alpha, \beta = x, y, z$. Quantities a , b , and d are the deformation potentials.

The second effect, considered here in more detail, is the appearance of k -linear terms in the Hamiltonian of electron and holes for crystals without inversion symmetry [24]:

$$\hat{H}_c^{(\varepsilon k)} = \frac{1}{2} \left(C_3 \sum_{\gamma} \sigma_{\gamma} \hat{\varphi}_{\gamma} + C'_3 \sum_{\gamma} \sigma_{\gamma} \hat{\psi}_{\gamma} \right), \quad (10)$$

$$\hat{H}_v^{(\varepsilon k)} = C_5 \sum_{\gamma} J_{\gamma} \hat{\varphi}_{\gamma} + C_6 \sum_{\gamma} J_{\gamma} \hat{\psi}_{\gamma} + C_7 \sum_{\alpha} J_{\gamma}^3 \hat{\varphi}_{\gamma} + C_8 \sum_{\gamma} J_{\gamma}^3 \hat{\psi}_{\gamma} + C_9 \sum_{\gamma} V_{\gamma} \hat{\chi}_{\gamma}, \quad (11)$$

where $\gamma = x, y, z$; quantities σ_{γ} are the Pauli matrices, $V_z = J_z(J_x^2 - J_y^2)$, and C_j, C'_j are material constants for a crystal under consideration ($j = 3, 4, \dots, 9$). Components of operators $\hat{\varphi}_{\gamma}$, $\hat{\psi}_{\gamma}$, and $\hat{\chi}_{\gamma}$ required for further consideration read

$$\begin{aligned} \hat{\varphi}_z &= \varepsilon_{xz} \hat{k}_x - \varepsilon_{yz} \hat{k}_y, \\ \hat{\psi}_z &= \hat{k}_z (\varepsilon_{xx} - \varepsilon_{yy}), \\ \hat{\chi}_z &= \hat{k}_z \left[\varepsilon_{zz} - \frac{1}{3} \text{Sp}(\varepsilon) \right]. \end{aligned} \quad (12)$$

Other (x and y) components of these operators can be obtained by the cyclic permutation of subscripts.

Analysis shows that to describe the phenomena under discussion, one should consider only terms $C_6 J_z \hat{\psi}_z$, $C_7 J_x^3 \hat{\varphi}_x$, $C_7 J_y^3 \hat{\varphi}_y$, and $C_8 J_z^3 \hat{\psi}_z$ (see Appendix A).

In what follows, we assume that pressure P is applied along axis x , which coincides with the C_4 ([100]) axis of the crystal lattice. Under such conditions, all of the off-diagonal components of the strain tensor are zero. The component of stress tensor u_{xx} is equal in magnitude to the applied pressure P and the diagonal components of strain tensor are described by expressions [29]

$$\begin{aligned} \varepsilon_{xx} &= S_{11} u_{xx} = S_{11} P, \\ \varepsilon_{yy} &= S_{12} u_{xx} = S_{12} P, \\ \varepsilon_{zz} &= S_{12} u_{xx} = S_{12} P, \end{aligned} \quad (13)$$

where $S_{\alpha\beta}$ are the components of the elastic compliance tensor.

Operators φ_x and φ_y are zero because they contain off-diagonal components ε_{xz} and ε_{yz} [see Eq. (12)], which are zero in the considered geometry. Therefore, only two terms, $C_6 J_z \hat{\psi}_z$, and $C_8 J_z^3 \hat{\psi}_z$, should be finally taken into account. The substitution of expressions (1) and (13) into Eq. (11) gives rise to the following expression for the stress-induced terms in the excitonic Hamiltonian:

$$\hat{H}^{(K\varepsilon)} = \frac{m_h}{M} (C_6 J_z + C_8 J_z^3) (S_{11} - S_{12}) P \hat{K}_z. \quad (14)$$

This operator calculated using wave functions (8) is the 8×8 diagonal matrix. Its nonzero matrix elements have the form

$$\begin{aligned} H_{j+s, j+s}^{(K\varepsilon)} &= A_j K, \\ A_j &\equiv \frac{m_h}{M} (j C_6 + j^3 C_8) (S_{11} - S_{12}) P, \end{aligned} \quad (15)$$

where $j = \pm 3/2, \pm 1/2$ and $s = \pm 1/2$. Note that the sign of constant A_j is determined by the sign of the angular momentum projection j for the hole so that $A_j = -A_{-j}$. Parameters C_6 and C_8 can be determined using expressions given in Ref. [24]. Analysis shows that $A_{\pm 1/2} = 0$ for the light-hole exciton in all crystals with zinc-blende structure. Quantity $A_{\pm 3/2}$ describing the effect of K -linear terms for the heavy-hole exciton is completely determined by the applied stress and by material parameters. Its value for the QW under consideration is given in Sec. III.

Let us now consider in more detail the effects described by the Bir-Pikus Hamiltonian (9). At the chosen direction [100] of applied stress, this Hamiltonian reads

$$\hat{H}_\varepsilon = -a\mathbb{I}\text{Sp}(\varepsilon) + b \sum_{\alpha} J_{\alpha}^2 \left[\varepsilon_{\alpha\alpha} - \frac{1}{3}\text{Sp}(\varepsilon) \right], \quad (16)$$

where $\varepsilon_{xx}, \varepsilon_{yy}, \varepsilon_{zz}$ are described by expressions (13).

In addition to the shift of valence band, this Hamiltonian describes the mixing of heavy and light holes, since matrices J_x^2 and J_y^2 contain off-diagonal elements. This mixing is significant because deformation potentials a and b are large. In particular, they are in orders of magnitude larger than the matrix elements of Hamiltonian (14) for the actual range of wave vectors $K (0 \div 5 \times 10^6 \text{ cm}^{-1})$.

Finally, the total excitonic Hamiltonian in the presence of uniaxial stress consists of Hamiltonians (7), (14), and (16). This Hamiltonian does not mix optically active states, $|j, s\rangle = |\pm 3/2, \mp 1/2\rangle, |\pm 1/2, \pm 1/2\rangle$, with optically inactive states, $|j, s\rangle = |\pm 3/2, \pm 1/2\rangle, |\pm 1/2, \mp 1/2\rangle$, as it follows from the properties of matrices $J_x, J_x^3, J_x^2, J_y^2, J_z^2$ (see, e.g., [25]). Therefore, we further restrict our analysis only by the bright excitons. The matrix of the total exciton Hamiltonian built on the wave functions of the bright exciton has the form

$$\hat{H}_X = \hat{H}_X^{(0)} + \hat{H}^{(K\varepsilon)} + \hat{H}_\varepsilon = \begin{pmatrix} H_{h+} & 0 & V & 0 \\ 0 & H_{l+} & 0 & V \\ V & 0 & H_{l-} & 0 \\ 0 & V & 0 & H_{h-} \end{pmatrix}, \quad (17)$$

where

$$H_{h\pm} = H_{Xh}^{(0)} + H_{\varepsilon h} \pm A_{3/2} K,$$

$$H_{l\pm} = H_{Xl}^{(0)} + H_{\varepsilon l},$$

$$V = \frac{3}{2} b (S_{11} - S_{12}) P,$$

$$H_{\varepsilon h, l} = -a \text{Sp}(\varepsilon) \pm \frac{b}{2} (\varepsilon_{xx} + \varepsilon_{yy} - 2\varepsilon_{zz}).$$

In the last expression, the upper signs refer to the heavy-hole excitons, while the lower ones refer to the light-hole excitons.

The exciton wave function for this problem is constructed as a linear combination of the basic wave functions (8),

$$\Psi(K) = \sum_{j,s} C_{j,s} |j,s\rangle, \quad (18)$$

where $C_{j,s}$ are the expansion coefficients.

III. PERMITTIVITY TENSOR

For calculation of the reflection spectra in the presence of the pressure-induced effects, we use the model of interference of the bulk polariton waves described in Refs. [22,23]. We consider the model of a heterostructure consisting of the QW layer surrounded by semi-infinite barriers. We assume that the incident light propagates perpendicularly to the QW and has a circular polarization. The latter corresponds to the creation of an exciton with a certain projection of the angular momentum on the direction of propagation.

For further analysis, we consider the wave to be right-hand polarized if the projection of the photon angular momentum onto the chosen axis Z is $+1$ and to be left-hand polarized if this projection is -1 . With this definition, the sign of the circular polarization is not changed when the propagation of light is changed to the opposite direction. Such a definition is convenient when writing the boundary conditions for exciton polaritons; see next section. It should be emphasized that this definition does not match with the commonly used one for the polarization, which is determined by the angular momentum projection of photons on the direction of propagation and, therefore, is reversed under reflection.

As the first step, we should calculate the permittivity tensor of the medium, $\epsilon(\omega, K)$, taking into account the exciton-photon interaction. Tensor $\epsilon(\omega, K)$ is the 3×3 matrix describing two transverse and one longitudinal modes. However, under normal incidence of light, only transverse modes are excited in the crystal, and the 2×2 permittivity tensor is relevant to this case.

The exciton-photon interaction is described by the perturbation operator ([30,31]),

$$(d_h^{(\pm)} + d_l^{(\pm)})E^{(\pm)}, \quad (19)$$

where $E^{(\pm)}$ is the electric-field amplitude of the light wave and superscript “ \pm ” corresponds to two circular polarizations of light. The matrix element of the dipole moment operator, $\hat{d}_{\pm} = e(x \pm y)$, has the form ([30,31])

$$d_h^{(\pm)} = \langle 0 | \hat{d}^{(\pm)} | \pm 3/2, \mp 1/2 \rangle,$$

$$d_l^{(\pm)} = \langle 0 | \hat{d}^{(\pm)} | \pm 1/2, \pm 1/2 \rangle.$$

Wave function $|0\rangle$ describes the vacuum state of a crystal that is the state with no exciton. For both circular polarizations, $|d_{h,l}^{(+)}| = |d_{h,l}^{(-)}| = d_{h,l}$, where $d_h^2 = 3d_l^2 = \frac{3}{4}\hbar\omega_{LT}\epsilon_0$ is the squared matrix element of the dipole moment normalized to unit volume. Quantity $\hbar\omega_{LT}$ is the energy of longitudinal-transverse splitting describing the strength of the exciton-photon interaction.

The exciton-photon interaction changes polarization of the medium, which is described by the expression [30,31]

$$\mathcal{P}^{(\pm)} = d_h C_{\pm 3/2, \mp 1/2} + d_l C_{\pm 1/2, \pm 1/2}, \quad (20)$$

where $C_{j,s}$ are the expansion coefficients in expression (18). Polarization vector \mathcal{P} is associated with vector $E^{(\pm)}$ via electric susceptibility tensor $4\pi\chi_{\alpha\beta}$:

$$\mathcal{P}^{(\pm)} = 4\pi\chi_{\pm\pm}E^{(\pm)} + 4\pi\chi_{\pm\mp}E^{(\mp)}.$$

The dispersion relations, the wave functions, and the permittivity tensor of the medium in the presence of the exciton-photon interaction can be found using the method proposed in Refs. [30,31]. To this end, one should first solve a system of equations for the energies of the four states with perturbation (19) (see, e.g., [31]),

$$(\mathbb{H} - \mathbb{I}\hbar\omega)\mathbb{C} = 0, \quad (21)$$

where $\hbar\omega$ is the photon energy, and matrix $(\mathbb{H} - \mathbb{I}\hbar\omega)$ and vector \mathbb{C} have the form

$$(\mathbb{H} - \mathbb{I}\hbar\omega) = \begin{pmatrix} H_{h+} - \hbar\omega & 0 & V & 0 & d_h & 0 \\ 0 & H_{l+} - \hbar\omega & 0 & V & d_l & 0 \\ V & 0 & H_{l-} - \hbar\omega & 0 & 0 & d_l \\ 0 & V & 0 & H_{h-} - \hbar\omega & 0 & d_h \end{pmatrix}, \quad \mathbb{C} = \begin{pmatrix} C_{+3/2, -1/2} \\ C_{+1/2, +1/2} \\ C_{-1/2, -1/2} \\ C_{-3/2, +1/2} \\ -E^{(+)} \\ -E^{(-)} \end{pmatrix}. \quad (22)$$

Coefficients $C_{j,s}$ can be found solving system (22):

$$C_{\pm 3/2, \mp 1/2} = \frac{\tilde{H}_{l\mp} d_h E^{(\pm)}}{\tilde{H}_{h\pm} \tilde{H}_{l\mp} - V^2} - \frac{V d_l E^{(\mp)}}{\tilde{H}_{l\mp} \tilde{H}_{h\pm} - V^2}, \quad (23)$$

$$C_{\pm 1/2, \pm 1/2} = \frac{\tilde{H}_{h\mp} d_l E^{(\pm)}}{\tilde{H}_{l\pm} \tilde{H}_{h\mp} - V^2} - \frac{V d_h E^{(\mp)}}{\tilde{H}_{l\pm} \tilde{H}_{h\mp} - V^2}. \quad (24)$$

Here, $\tilde{H}_{\alpha} \equiv H_{\alpha} - \hbar\omega + i\Gamma$, where Γ is a phenomenological parameter introduced to describe the processes of energy dissipation. Substituting (23) and (24) into Eq. (20), we

obtain

$$\frac{\tilde{H}_{l\mp} d_h^2 E^{(\pm)}}{\tilde{H}_{h\pm} \tilde{H}_{l\mp} - V^2} + \frac{\tilde{H}_{h\mp} d_l^2 E^{(\pm)}}{\tilde{H}_{l\pm} \tilde{H}_{h\mp} - V^2} - \frac{V d_l d_h E^{(\mp)}}{\tilde{H}_{l\mp} \tilde{H}_{h\pm} - V^2} - \frac{V d_l d_h E^{(\mp)}}{\tilde{H}_{l\pm} \tilde{H}_{h\mp} - V^2} = 4\pi\chi_{\pm\pm}E^{(\pm)} + 4\pi\chi_{\pm\mp}E^{(\mp)}. \quad (25)$$

This relation allows one to finally obtain relations for components $\chi_{\alpha\beta}$:

$$4\pi\chi_{\pm\pm} = \frac{\tilde{H}_{l\mp} d_h^2}{\tilde{H}_{h\pm} \tilde{H}_{l\mp} - V^2} + \frac{\tilde{H}_{h\mp} d_l^2}{\tilde{H}_{l\pm} \tilde{H}_{h\mp} - V^2}, \quad (26)$$

and

$$4\pi\chi_{+-} = 4\pi\chi_{-+} = -\frac{Vd_id_h}{\tilde{H}_{l\mp}\tilde{H}_{h\pm} - V^2} - \frac{Vd_hd_l}{\tilde{H}_{l\pm}\tilde{H}_{h\mp} - V^2}. \quad (27)$$

Beside the effects related to excitons, the uniaxial stress leads to a piezo-optical effect, due to which the isotropic crystal becomes uniaxial. In our case, the principal optical axis of the crystal is perpendicular to the direction of light propagation. In the basis of circularly polarized light waves, this effect can be described by additional diagonal and off-diagonal terms in the permittivity tensor, which have the form [32]

$$\begin{aligned} \delta\epsilon_{++} &= \delta\epsilon_{--} = (\pi_{11} + \pi_{12})P/2, \\ \delta\epsilon_{+-} &= \delta\epsilon_{-+} = (\pi_{11} - \pi_{12})P/2. \end{aligned} \quad (28)$$

Here π_{11}, π_{12} are components of the background piezo-optic tensor, whose values can be found in the literature (see, e.g., [32]).

The total permittivity is expressed in terms of the electric susceptibility (26) and (27) as follows:

$$\epsilon_{\pm\pm}(\omega, K) = \epsilon_0 + \delta\epsilon_{\pm\pm} + 4\pi\chi_{\pm\pm}, \quad (29)$$

$$\epsilon_{+-}(\omega, K) = \epsilon_{-+}(\omega, K) = \delta\epsilon_{+-} + 4\pi\chi_{+-}. \quad (30)$$

The permittivity tensor in the basis of circular polarizations has the form

$$\epsilon(\omega, K) = \begin{pmatrix} \epsilon_{++} & \epsilon_{+-} \\ \epsilon_{-+} & \epsilon_{--} \end{pmatrix}. \quad (31)$$

It is easy to verify that for the diagonal matrix elements of the tensor, the following relation is valid:

$$\epsilon_{++}(\omega, K) = \epsilon_{--}(\omega, -K). \quad (32)$$

This relation is equivalent to the a well-known relation [33]

$$\epsilon_{xy}(\omega, K) = \epsilon_{yx}(\omega, -K), \quad (33)$$

where $\epsilon_{xy}, \epsilon_{yx}$ are components of the permittivity tensor in the basis of linearly polarized waves. They are related to

components (29) and (30) by well-known formulas (see, e.g., [34]):

$$\epsilon_{xy}(\omega, K) = -\epsilon_{yx}(\omega, K) = i\frac{1}{2}[\epsilon_{++}(\omega, K) - \epsilon_{--}(\omega, K)]. \quad (34)$$

First, we use resulting expression (31) for calculation of the dispersion relations for polariton eigenmodes. To this end, we solve the dispersion equation [33]

$$\epsilon(\omega, K) = \mathbb{I} \frac{c^2 K^2}{\omega^2}, \quad (35)$$

where c is the light velocity and $\epsilon(\omega, K)$ is the permittivity described by expressions (29)–(31).

Equation (35) has 12 independent solutions for dispersion relations $K_i(\omega)$, half of which correspond to the propagation of polariton waves in the forward direction and the other half correspond to the backward one. The eigenmodes differ from each other by the predominant contribution of the photonlike (p -type) or excitonlike (l - and h -type) components; see Fig. 1. Since permittivity tensor (31) has nonzero off-diagonal matrix elements, all of the eigenmodes propagating in the strained crystal, in general, are elliptically polarized. In particular, six waves are predominantly left-hand polarized, while the other six are right-hand polarized.

Figure 1 shows the dispersion curves for polariton eigenmodes calculated for a GaAs crystal. The following material parameters are used: $\hbar\omega_{LT} = 0.09$ meV [35], $\epsilon_0 = 12.56$ [36], $m_e = 0.067m_0$ [37], $m_{hh} = 0.45m_0$, $m_{lh} = 0.082m_0$ [38] (m_0 is the free-electron mass), $E_g = 1520$ meV [39], $R = 5$ meV, $S_{11} = 1.76 \times 10^{-12}$ cm²/dyn and $S_{12} = -0.37 \times 10^{-12}$ cm²/dyn [40], $\pi_{11} = 0.2$ GPa⁻¹, $\pi_{12} = 0.05$ GPa⁻¹, $\pi_{11} - \pi_{12} \approx 0.2$ GPa⁻¹ [32], and $a = -6.7$ eV, $b = -1.7$ eV [28]. Constants C_6 and C_8 are calculated using formulas and material constants given in Ref. [24]: $C_6 = -1$ meV/cm and $C_8 = -4$ meV/cm. The value of the damping parameter has been chosen to obtain the width of oscillations in the calculated reflection spectra (see below) approximately equal to that typically observed in the experiment: $\Gamma = 0.05$ meV. The figure shows the dispersion curves for pressure $P = 0$ and $P = 1$ GPa. Since the GaAs crystal is destroyed at larger

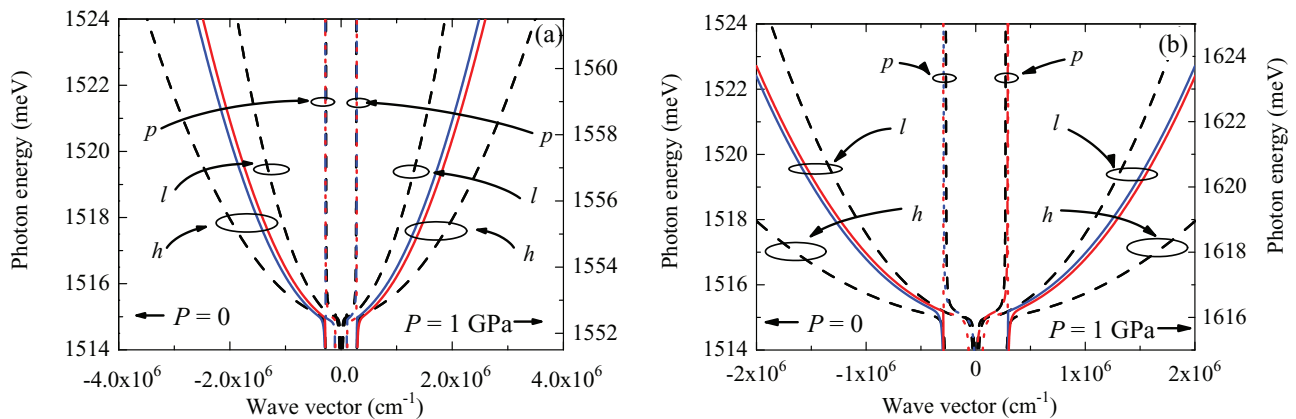


FIG. 1. (Color online) The change of the dispersion relations of (a) h -polariton and (b) l -polariton branches under pressure $P = 1$ GPa. Black dashed lines are the initial dispersion curves at $P = 0$. Red and blue lines represent polariton modes with dominant right-hand and left-hand circularly polarized components in the stressed crystal, respectively. Legends h , l , and p are explained in the text. The left and right energy scales correspond to cases $P = 0$ and $P = 1$ GPa.

uniaxial stress [41,42], the pressure effects at $P > 1$ GPa were not considered.

As seen in Fig. 1, the strain results in two main effects. The first one is the change of curvature of the excitonlike dispersion branches. It is caused by mixing of the heavy-hole and light-hole exciton states and is described by the off-diagonal matrix element V in matrix (22). Dispersion curves for h -type waves, which correspond to the heavy-hole excitons in the absence of strain, become steeper with increasing pressure [see Fig. 1(a)] and those for the l -type waves initially corresponding to light-hole excitons become flatter [Fig. 1(b)]. This effect can be treated as the convergence of the effective masses of excitons of the h and l types.

The second effect is the antisymmetric in K splitting of dispersion branches of h and l types, which is described by term (15) in the exciton Hamiltonian. If $K > 0$, the dispersion branch for the right-hand polarization is higher in energy than the branch for the left-hand polarized component. If $K < 0$, these branches are swapped [see Fig. 1(a)]. The relatively weak, at first glance, splitting of the dispersion curves leads to a qualitatively new effect in the reflection spectra of the QW.

IV. BOUNDARY CONDITIONS

To formulate the boundary conditions, one should obtain a relation between the electric fields $E_\rho^{(+)}$ and $E_\rho^{(-)}$ for polariton eigenmodes. The relation follows from Eqs. (31) and (35):

$$\mathbb{I} \frac{c^2 K_\rho^2}{\omega^2} \mathbb{E}_\rho = \epsilon(\omega, K_\rho) \mathbb{E}_\rho, \quad (36)$$

where the vector

$$\mathbb{E}_\rho = \begin{pmatrix} E_\rho^{(+)} \\ E_\rho^{(-)} \end{pmatrix}$$

describes the elliptical polarization of the eigenmode ρ . Subscript ρ includes three components,

$$\rho = \{\lambda, d, e\},$$

where $\lambda = p, l, h$ indicates the type of the eigenmode, and $d = \rightarrow$ or \leftarrow shows the direction of wave propagation. Index “ e ” specifies the ellipticity, in particular, $e = right$ denotes the wave with a prevailing right-hand circularly polarized component, and $e = left$ is the wave with a prevailing left-hand polarized component (see Fig. 1).

Substitution of vector \mathbb{E}_ρ in expression (36) provides a relation between the circularly polarized components,

$$\frac{c^2 K_\rho^2}{\omega^2} E^{(\pm)} = \epsilon_{\pm\pm} E_\rho^{(\pm)} + \epsilon_{+-} E_\rho^{(\mp)}, \quad (37)$$

which can be written as

$$E_\rho^{(\pm)} = \xi_\rho^{(\mp)} E_\rho^{(\mp)}, \quad (38)$$

where

$$\xi_\rho^{(\pm)} = \frac{\epsilon_{+-}(\omega, K_\rho)}{\epsilon_{\pm\pm}(\omega, K_\rho) - n_\rho^2(\omega, K_\rho)}.$$

The polariton eigenmodes propagating in the optically uniaxial QW are shown in Fig. 2. The circularly polarized incident

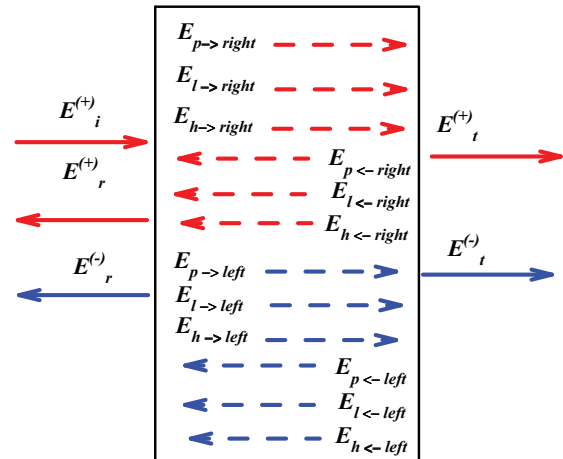


FIG. 2. (Color online) Polaritonic eigenmodes in the QW layer. Red dashed arrows indicate polariton waves with predominant σ^+ polarization (subscript *right*). Blue dashed arrows show the polariton waves with a predominant σ^- polarization (subscript *left*). The solid red and blue arrows indicate the light waves in copolarizations and cross polarizations, respectively, passed through and reflected from the QW.

light can excite all modes, but with different efficiency. The reflected light, in general, is elliptically polarized, i.e., can be decomposed into two circularly polarized components. Therefore, two sets of boundary conditions should be considered for each heterointerface, with one set per each circular polarization. In what follows, we assume that the incident light has the right-hand helicity.

Boundary conditions include the Maxwell's conditions, which require continuity of the tangential components of electric $E^{(\pm)}$ and magnetic $B^{(\pm)}$ fields of polaritonic waves at the QW heterointerfaces. For plane waves, the magnetic induction can be expressed in terms of the electric-field amplitude, $B_\rho^{(\pm)} = n_\rho E_\rho^{(\pm)}$, where refractive index $n_\rho = cK_\rho/\omega$. Thus, if there are incident, transmitted, and reflected waves at the QW heterointerfaces, the boundary conditions for the circularly polarized components can be written as

$$\begin{aligned} E_i^{(+)} e^{iqZ_{1,2}} + E_g^{(+)} e^{-iqZ_{1,2}} &= \sum_\rho E_\rho^{(+)} e^{iK_\rho Z_{1,2}}, \\ n_0 E_i^{(+)} e^{iqZ_{1,2}} - n_0 E_g^{(+)} e^{-iqZ_{1,2}} &= \sum_\rho n_\rho E_\rho^{(+)} e^{iK_\rho Z_{1,2}}, \end{aligned} \quad (39)$$

and

$$\begin{aligned} E_g^{(-)} e^{-iqZ_{1,2}} &= \sum_\rho E_\rho^{(-)} e^{iK_\rho Z_{1,2}}, \\ -n_0 E_g^{(-)} e^{iqZ_{1,2}} &= \sum_\rho n_\rho E_\rho^{(-)} e^{iK_\rho Z_{1,2}}, \end{aligned} \quad (40)$$

where $E_i^{(\pm)}$, $E_r^{(\pm)}$ are the amplitudes of the circularly polarized components of the incident, reflected ($g = r$), or transmitted ($g = t$) light waves outside the QW. Quantities n_0 and q are the refractive index and the modulus of the wave vector of light in barriers, respectively. Coordinates $Z_1 = 0$ and $Z_2 = L_{\text{QW}}$ correspond to the boundaries of the QW.

Besides the Maxwell's boundary conditions, we use the Pekar's additional boundary conditions (ABC). According to them, the polarization of the crystal caused by the heavy-hole and light-hole excitons vanishes at the boundaries of the QW (see Ref. [30]). Since their contribution is described by expression (20), the ABC can be written as

$$\sum_{\rho} d_h C_{\pm 3/2, \mp 1/2}(K_{\rho})|_{L=0, L_{\text{QW}}} = 0, \quad (41)$$

$$\sum_{\rho} d_l C_{\pm 1/2, \pm 1/2}(K_{\rho})|_{L=0, L_{\text{QW}}} = 0,$$

where ρ runs over all polaritonic modes. Using expressions (23) and (24) for coefficients $C_{\pm 3/2, \mp 1/2}$ and $C_{\pm 1/2, \pm 1/2}$, we obtain four ABC at each boundary:

$$\sum_{\rho} \frac{d_h^2 \tilde{H}_{l\mp}(K_{\rho}) E_{\rho}^{(\pm)} e^{iK_{\rho} Z_{1,2}}}{\tilde{H}_{h\pm}(K_{\rho}) \tilde{H}_{l\mp}(K_{\rho}) - V^2} - \sum_{\rho} \frac{d_l d_h V E_{\rho}^{(\mp)} e^{iK_{\rho} Z_{1,2}}}{\tilde{H}_{h\pm}(K_{\rho}) \tilde{H}_{l\mp}(K_{\rho}) - V^2} = 0, \quad (42)$$

$$\sum_{\rho} \frac{d_l^2 \tilde{H}_{h\mp}(K_{\rho}) E_{\rho}^{(\pm)} e^{iK_{\rho} Z_{1,2}}}{\tilde{H}_{l\pm}(K_{\rho}) \tilde{H}_{h\mp}(K_{\rho}) - V^2} - \sum_{\rho} \frac{d_h d_l V E_{\rho}^{(\mp)} e^{iK_{\rho} Z_{1,2}}}{\tilde{H}_{l\pm}(K_{\rho}) \tilde{H}_{h\mp}(K_{\rho}) - V^2} = 0. \quad (43)$$

It is easy to see that at zero pressure, when $V = 0$, these ABC are transformed into the ordinary Pekar's ABC.

V. REFLECTANCE SPECTRA

Boundary conditions (39)–(43) comprise a system of linear equations for amplitudes of the electric field of light waves and of polariton waves in the structure. Solution of this system allows one to determine amplitudes of the incident and reflected light waves in two polarizations and to calculate reflection coefficients:

$$R^{(++)}(\omega) = \frac{|E_i^{(+)}|^2}{|E_r^{(+)}|^2},$$

$$R^{(-+)}(\omega) = \frac{|E_i^{(-)}|^2}{|E_r^{(+)}|^2},$$

where superscripts “++” and “-+” denote the reflection coefficients in the copolarization and cross polarization. We have carried out calculations of reflection spectra for the GaAs QW with thickness $L_{\text{QW}} = 700$ nm. Background permittivity of the left and right semi-infinite space were chosen to be $\epsilon_l = 1$ and $\epsilon_r = 11$, which correspond to the air permittivity on the left side and to a typical semiconductor one on the right side.

The copolarized reflectance spectra calculated in the framework of the described model are shown in Figs. 3 and 4. Each spectrum contains intense peaks and quasiperiodic oscillations. The peaks correspond to the anticrossing of the photon and exciton dispersion branches, while the oscillations are due to the interference of the excitonlike and photonlike

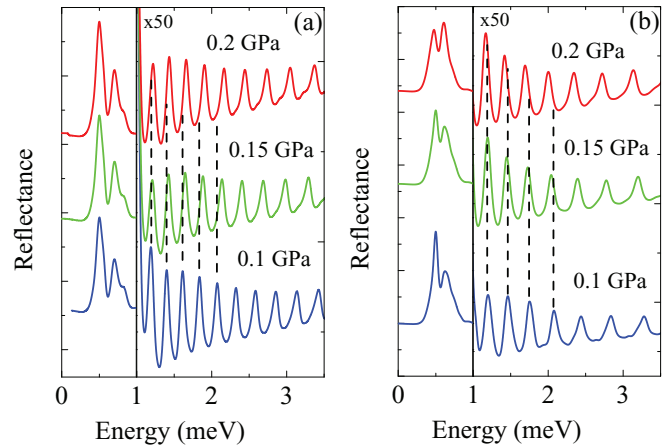


FIG. 3. (Color online) Reflection spectra $R^{(++)}(\omega)$ for the GaAs QW with $L_{\text{QW}} = 700$ nm in the spectral range of interference of the (a) h -polariton and (b) l -polariton modes. The magnitude of the applied pressure is given near respective curves. The spectra are shifted along the energy axis to match their dominant features. The energy of dominant features is taken to be zero. If $P = 0$, its value $E \approx 1515$ meV. The dashed vertical lines allow one to demonstrate the relative shift of the oscillations. The amplitude of spectral oscillation is multiplied by 50.

modes. The spectra of l -type polaritons are strongly shifted to a higher energy range at pressure $P > 0.1$ GPa and are not overlapped with those of h -type polaritons. Therefore, they can be analyzed separately. As seen in Fig. 3(a), the distance between the spectral oscillations for h polaritons becomes larger with increasing pressure, which is a result of the aforementioned decrease of the effective mass (see Fig. 1). Correspondingly, the spectral oscillations for l polaritons become denser [see Fig. 3(b)] due to the increasing mass of the l -type excitons. The pressure dependences of masses for h and l excitons obtained from analysis of the curvature of dispersion branches are shown in Fig. 5.

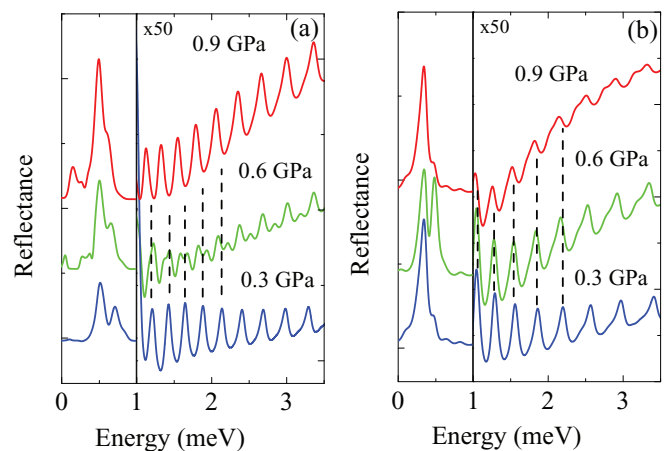


FIG. 4. (Color online) Reflection spectra $R^{(++)}(\omega)$ at pressure $P > 0.3$ GPa in the spectral range of the (a) h -polariton and (b) l -polariton modes, respectively. Other notations are the same as in Fig. 3.

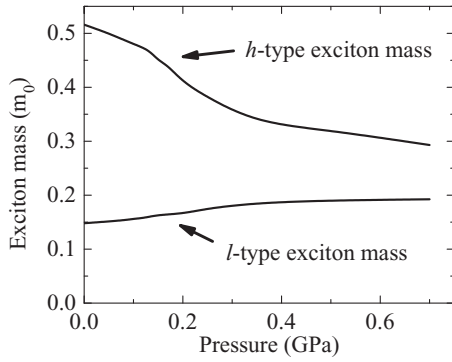


FIG. 5. Exciton masses in the GaAs crystal as functions of the applied pressure.

At larger pressures, $P \geq 0.3$ GPa, the “stretching” or “compressing” of the oscillations is no longer observed; see Fig. 4.

To discuss this behavior of oscillations qualitatively, we neglect the exciton-photon interaction and calculate the exciton energy from the secular equation with the Hamiltonian (17),

$$\det |\hat{H}_X - E\mathbb{I}| = 0.$$

Let us denote $\Theta \equiv (\frac{\hbar^2}{2M_h} - \frac{\hbar^2}{2M_l})$ and $\Delta \equiv (H_{\varepsilon h} - H_{\varepsilon l}) = b(\varepsilon_{xx} + \varepsilon_{yy} - 2\varepsilon_{zz})$. Note that the K -linear terms of the Hamiltonian are small in comparison with $\Theta K^2, V, \Delta$, so that one may neglect term $A_{3/2}K$ in Hamiltonian (17). In this approximation, the energy of the l and h excitons is

$$E_{\pm} = \frac{1}{2}[(H_{h\pm} + H_{l\mp}) \pm \sqrt{(H_{h\pm} - H_{l\mp})^2 + 4V^2}] \\ \approx \frac{1}{2}[(H_{h\pm} + H_{l\mp}) \pm \sqrt{(\Theta K^2 + \Delta)^2 + 4V^2}].$$

Note that quantities Δ and V linearly depend on the pressure. At small pressure, when ΘK^2 is of the same order as Δ and V , the exciton energy essentially depends on the wave vector, resulting in a relatively fast convergence of exciton masses (see Fig. 5) and, correspondingly, in stretching and compressing of the h and l oscillations, respectively. At high pressure, Δ and V are large compared with ΘK^2 and this term can be neglected. Therefore, the convergence of the masses and modification of the oscillations are blocked at high pressures, as can be seen in Figs. 4 and 5.

At pressure $P \geq 0.4$ GPa, another effect appears, which is caused by the K -linear splitting of dispersion branches already demonstrated in Fig. 1. As seen in Fig. 4(a), the oscillations in the h spectrum decrease in amplitude with increasing pressure. However, at pressure above a certain critical value, P_{cr} , the oscillations begin to recover, their phase being opposite to that at low pressures. This phenomenon can be called an “inversion” of the oscillation phase. It should be emphasized that the amplitude of the dominant reflection peak is almost independent of the pressure.

Analysis showed that P_{cr} is a function of the QW width, L_{QW} . It is approximately inversely proportional to L_{QW} and, for the GaAs QW, is fitted by dependence: $P_{cr} = a + b/L_{QW}$ with $a = -0.3$ GPa, and $b = 480$ GPa/nm. Note that for $L_{QW} < 400$ nm, the critical pressure exceeds the ultimate magnitude for the GaAs crystal [41,42]. Nevertheless, since the spectral oscillations are observable in the high-quality GaAs

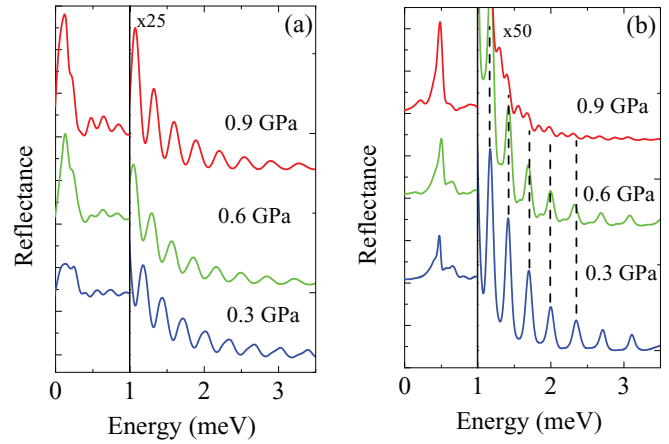


FIG. 6. (Color online) Reflection spectra in cross polarization in spectral range of interference of (a) h -polariton and (b) l -polariton modes. Other notations are the same as in Fig. 3.

QWs with thickness up to 1 micron (see Ref. [23]), there is a real possibility to see this effect experimentally.

The phase inversion in the l spectrum appears at higher pressures [see Fig. 4(b)]. The reason for that is the absence of K -linear splitting for the basic light-hole exciton states [see Eq. (15)]. However, the admixture of the heavy-hole exciton states at high pressures may result in the K -linear splitting and, correspondingly, in the inversion of the oscillations phase. A detailed discussion of the origin of phase inversion is presented in the next section.

Let us consider the cross-polarized components of the h and l spectra calculated for the same QW (Fig. 6). Their amplitudes are determined by nondiagonal components of the permittivity tensor [see Eqs. (27), (30), and (37)], which, in turn, is determined by the perturbation V ; see Eq. (17). The amplitude of spectral oscillations rapidly decreases with increasing photon energy in a few meV. Note that in copolarization, the oscillation amplitude does not decrease noticeably in the same spectral range; see Fig. 3. This difference is due to a rapid divergence of the h - and l -dispersion branches with the wave vector increase and, correspondingly, to a rapid decrease of mixing of the light-hole and heavy-hole excitons.

The inversion of the phase of the oscillations is not observed in the cross-polarized h spectrum; see Fig. 6(a). The reason is that these spectra are caused by the strain-induced admixture of the light-hole excitons whose Hamiltonian does not contain K -linear terms [see Eq. (17)]. On the contrary, the cross-polarized l spectra do reveal the phase inversion effect [Fig. 6(b)] at pressures even lower than that for the copolarized l spectra [cf. with Fig. 4(b)]. This is due to the admixture of heavy-hole excitons, which are K -linearly split.

To conclude this section, we should note that even at the maximum possible pressure $P = 1$ GPa, the spectral amplitude of copolarized and cross-polarized oscillations is comparable in magnitude only in a small spectral range of about 0.5 meV above the exciton transition. At higher energies, the amplitudes of the cross-polarized oscillations become negligibly small. Thus, the effect of the circular polarizations’ conversion of incident light is negligible for

the rest of the spectrum. Therefore, this conversion effect is no longer considered in the next section.

VI. STRESS-INDUCED GYROTROPY

It follows from relation (32) that the uniaxial stress leads not only to birefringence, but also to gyrotropy. The gyrotropy is due to the K -linear splitting of the exciton states with positive and negative projections of the angular momentum on the Z axis (see, e.g., Refs. [10,12,13]). This splitting is described by expression (15). It should be emphasized that the necessary (though not sufficient) conditions for the appearance of gyrotropy are the lack of inversion symmetry and the presence of spatial dispersion of excitons [33].

The gyrotropy manifests itself in the appearance of ellipticity of the reflected light at the linearly and circularly polarized incident light. The ellipticity can be described by the ratio of major and minor axes of the polarization ellipse (E_b and E_s , respectively) and by the angle χ between the X axis and the direction of the major ellipse axis (see, e.g., [34]). The angle χ is determined by the expression

$$\chi = \arctan \left[\frac{-\mathcal{A} + \sqrt{\mathcal{B}^2 - 4\mathcal{A}\mathcal{C}}}{2\mathcal{A}} \right]. \quad (44)$$

Here, $\mathcal{A} = \text{Im}E_2 \cdot \text{Re}E_1 - \text{Re}E_2 \cdot \text{Im}E_1$, $\mathcal{B} = (\text{Re}E_2)^2 - (\text{Im}E_1)^2 + (\text{Im}E_2)^2 - (\text{Re}E_1)^2$, $\mathcal{C} = \text{Im}E_1 \cdot \text{Re}E_2 - \text{Re}E_1 \cdot \text{Im}E_2$, where $E_1 = E_r^{(+)} + E_r^{(-)}$ and $E_2 = E_r^{(+)} - E_r^{(-)}$. The ratio of major and minor axes is

$$e = \xi \frac{|E_x \cos(\chi) + i \cdot E_y \sin(\chi)|}{|-E_x \sin(\chi) + i \cdot E_y \cos(\chi)|}, \quad (45)$$

where $\xi = 1$ for $|E_r^{(+)}|/|E_r^{(-)}| > 1$ (right-hand elliptical polarization) and $\xi = -1$ for $|E_r^{(+)}|/|E_r^{(-)}| < 1$ (left-hand elliptical polarization).

We have calculated the spectra of $e(\omega)$ and $\chi(\omega)$ for h and l polaritons at pressure $P = 0.8$ GPa (Fig. 7). As seen, the

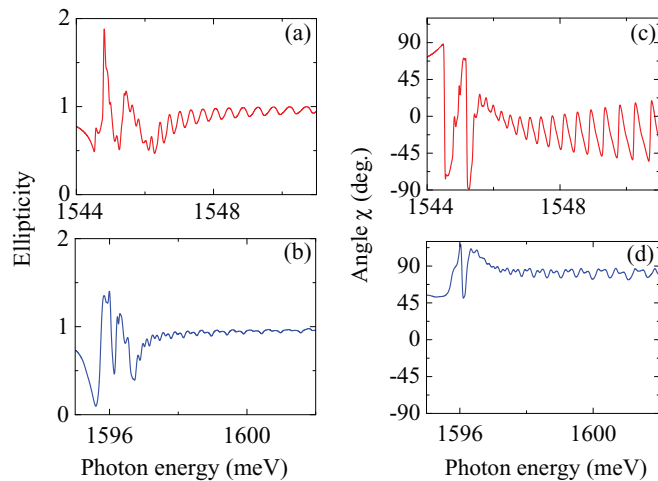


FIG. 7. (Color online) The spectra of (a), (b) the ellipticity $e(\omega)$ and (c), (d) angle $\chi(\omega)$ of the reflected light. Calculations are done for the GaAs QW with $L_{\text{QW}} = 700$ nm at $P = 0.8$ GPa for the spectral range of h - and l -polariton modes (red and blue curves, respectively). The incident light has the right circular polarization.

spectrum of $e(\omega)$ consists of a set of oscillations superimposed on the smoothly varying background. The magnitude of $e(\omega)$ significantly differs from unity only in the range of the anticrossing of exciton and photon dispersion curves. This is caused by the strong mixing of the photonlike and excitonlike modes in this range, which leads to a K -linear splitting of the photonlike branch. The ellipticity above the anticrossing is caused by the K -linear splitting only of the excitonlike branches.

Quantity $e(\omega)$ weakly oscillates in this spectral range about $+1$. The angle χ oscillates about zero for the h polariton and about $\pi/2$ for the l polariton. This means that the major axes of these excitons are perpendicular to each other. They swing about the direction of applied pressure (for the h polariton) and perpendicular to it (for the l polariton) as the light frequency is varied. The period of these oscillations coincides with that in the reflection spectra.

VII. DISCUSSION

In this section, we discuss in more detail specific mechanisms of the phase inversion of spectral oscillations. For simplicity, we consider the light-hole exciton; we restrict ourselves by the consideration of the heavy-hole exciton only. In this case, the Maxwell's boundary conditions and the Pekar's ABC are reduced to a simpler form described in Ref. [30]. We illustrate the mechanism of the phase inversion by calculations of the reflection spectra in framework of the multipath interference model described, e.g., in Ref. [34].

Let a circularly polarized light wave E_i fall onto the left boundary of a QW. This wave is partially reflected (wave $E_r^{(0)}$) and partially penetrates into the QW. In the QW layer, the excitonlike (E_x) and photonlike (E_p) polariton waves propagate in the forward direction along the Z axis. Amplitudes of waves $E_r^{(0)}$, E_x , and E_p are determined from the boundary conditions (B1). When the excitonlike wave E_x reaches the right interface of QW, it partially penetrates to the right barrier (wave E_x^t) and partially is reflected. After this reflection, two reflected waves, i.e., the excitonlike wave (E_{xx}) and the photonlike wave (E_{xp}), already propagate in the backward direction. Amplitudes of waves E_x^t , E_{xx} , and E_{xp} are also determined from the boundary conditions at the right interface. Similar processes occur with the photonlike wave E_p at the right boundary. Thus, four waves propagate from the right interface of the QW in the negative direction: E_{xx} , E_{xp} , E_{pp} , and E_{px} . Similarly, the waves E_{xx} , E_{xp} , E_{pp} , and E_{px} can partially penetrate into the left barrier and partially be reflected from the left barrier into the QW. After this reflection, eight waves propagate in the QW layer in the forward direction. These waves start a new cycle, as described above.

Thus, an infinite number of waves are generated in the QW during the propagation of light. The electric-field amplitudes of these waves can be expressed through E_i if the amplitude coefficients of reflection and transmission are known. However, it is technically difficult to sum all the possible contributions to the reflection because of the large number of waves created at each interface. However, our calculations show that to obtain a satisfactory agreement with the results obtained by the transfer-matrix method, it is enough to summarize a few main contributions into the reflected

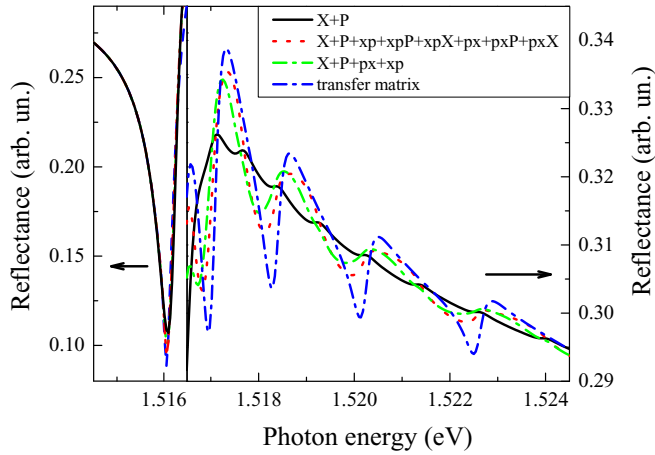


FIG. 8. (Color online) Reflection spectra calculated at $P = 0$. Solid curve is $|E_{r0} + E_{rP} + E_{rX}|^2$, rare dotted curve is $|E_{r0} + E_{rP} + E_{rX} + E_{rxp} + E_{rpx} + E_{rxpP} + E_{rpxX} + E_{rpxP} + E_{rpxX}|^2$, dash-dotted curve is $|E_{r0} + E_{rX} + E_{rP} + E_{rxp} + E_{rpx}|^2$, and the quick dotted line is the calculation method of transfer matrices. The amplitude of incident wave $|E_i| = 1$.

wave. Waves with similar subscripts can be summarized as an infinite geometric sequence. This allows one to find E_{rX} , E_{rxpX} , E_{rpxP} , E_{rpxX} , and E_{rpxP} , where capital subscripts

$$\begin{aligned}
 r &= \frac{E_{r0} + E_{rP} + E_{rX} + E_{rxp} + E_{rpx}}{E_i} = r_{00} + \frac{t_{p0}^- r_{pp}^{+-} t_{0p}^+ e^{i(K_{p-} + K_{p+})L_{QW}}}{1 - r_{pp}^{+-} r_{pp}^{+-} e^{i(K_{p-} + K_{p+})L_{QW}}} \\
 &+ \frac{t_{x0}^- r_{xx}^{+-} t_{0x}^+ e^{i(K_{x-} + K_{x+})L_{QW}}}{1 - r_{xx}^{+-} r_{xx}^{+-} e^{i(K_{x-} + K_{x+})L_{QW}}} + t_{p0}^- r_{xp}^{+-} t_{0x}^+ e^{i(K_{x+} + K_{p-})L_{QW}} + t_{x0}^- r_{px}^{+-} t_{0p}^+ e^{i(K_{x-} + K_{p+})L_{QW}} \\
 &\approx r_{00} + \frac{A_P e^{2iK_{p0}L_{QW}}}{1 - B_P e^{2iK_{p0}L_{QW}}} + \frac{A_X e^{2iK_{x0}L_{QW}}}{1 - B_X e^{2iK_{x0}L_{QW}}} + 2A_{xp} e^{i(K_{x0} + K_{p0})L_{QW}} \cos \frac{\Delta K_x L_{QW}}{2}, \quad (46)
 \end{aligned}$$

where conversion coefficients r_{00} , t_{0p}^+ , t_{0x}^+ are given in Appendix X [see Eq. (B2)], and the other coefficients are calculated in a similar way.

Equation (46) allows one to understand the effect of the inversion of the oscillation phase. When the last term is zero, i.e., $\cos(\Delta K_x L_{QW}/2) = 0$, the oscillations disappear. It follows that the critical pressure is

$$P_{cr} = \frac{\pi \hbar^2}{2m_h(|j|C_6 + |j|^3 C_8)(S_{11} - S_{12})L_{QW}},$$

where $j = 3/2$, and other notations are the same as in Eqs. (11) and (13). Below this pressure, $\cos(\Delta K_x L_{QW}/2) > 0$, the last term in Eq. (46) is positive and the oscillation phase has the same sign. Above it, $\cos(\Delta K_x L_{QW}/2) < 0$, and the sign is opposite.

The described effect of oscillation suppression at P_{cr} resembles the effect of suppression of the backscattering of carriers in two-dimensional (2D) topological insulators [15]. Indeed, the forward and backward propagation of carriers in the insulators gives rise to the destructive interference

indicate summation of an infinite number of similar waves, e.g., $E_{rxpX} = E_{rxpXX} + E_{rxpXXX} + \dots$.

Results of the calculation are shown in Fig. 8 for pressure $P = 0$. If only photonic waves E_{rP} and excitonic waves E_{rX} are taken into account, the calculated spectrum contains the main peak and almost nonoscillating background (solid line in the figure). Interference of waves E_{rxp} and E_{rpx} provides polariton oscillations, which spectral positions coincide with those calculated by the transfer-matrix method. Hence, the spectral oscillations are the result of the interference of the polaritonic waves, which propagate as photonlike waves in one direction and as excitonlike waves in the opposite direction, that is, E_{rxp} or E_{rpx} . That is the reason why the energy distance between the oscillation peaks is approximately two times larger than the distance between the neighboring energy levels of the exciton size quantization [23]. Extending the consideration to the waves E_{rxpP} , E_{rpxX} , E_{rpxP} , and E_{rpxX} improves agreement with the exact calculation, but does not provide any additional spectral features.

Upon application of pressure, the waves E_{rxp} and E_{rpx} are no longer equivalent: their amplitudes remain roughly the same, but the phases are different. Let us denote $\Delta K_x = (K_{x+} + K_{x-})/2$, $K_{x0} = (K_{x+} - K_{x-})/2$, and $K_{p+} \approx -K_{p-} \approx K_{p0}$, where K_{x0} and K_{p0} are the wave vectors at zero pressure. Note that wave vectors K_{x-} and K_{p-} are negative. The amplitude reflection coefficient, taking into account the major contributions, is

of their wave functions), which results in the suppression of backscattering. Similarly, the destructive interference of polaritonic waves in QWs almost totally suppresses the excitonlike polariton contribution into the reflection spectrum at P_{cr} .

VIII. CONCLUSION

We developed a theory of the interference of polariton modes in a heterostructure with a wide quantum well, subject to uniaxial stress perpendicular to the growth axis. The model includes the photon-exciton interaction and the strain-induced effects described by the Bir-Pikus Hamiltonian. In particular, the K -linear terms appearing in the hole Hamiltonian due to the strain are taken into account.

The first one is the convergence of masses of the heavy-hole and light-hole excitons with increasing pressure. The analysis shows that this effect is due to mixing of these excitons, which is described by the Hamiltonian of Bir and Pikus.

Another effect of deformation is the suppression of oscillations in the spectra of the circularly copolarized reflection

at some critical pressure and their recovery when the pressure increases further. This effect is accompanied by the inversion of the oscillation phase. The phenomenon is a direct consequence of a more general effect of the K -linear splitting of the valence band Γ_8 that is induced in crystals without the inversion symmetry by a uniaxial stress.

The analysis shows that in spectra of the circularly cross-polarized reflection, the spectral oscillations can also be observed. The amplitude of these oscillations increases with the increasing pressure. However, even at the highest possible pressure, the amplitude of these oscillations is much smaller than that of oscillations in the copolarized reflection. The effect of phase inversion for light-hole excitons also can be observed due to the mixing with the heavy-hole excitons, but it occurs at higher pressures.

The estimates made in this paper show that the considered effects can be experimentally observed in heterostructures with relatively wide GaAs/AlGaAs quantum wells at subcritical pressures $P < 1$ GPa, at which the crystal is not yet damaged.

ACKNOWLEDGMENTS

We appreciate valuable discussions with I. Ya. Gerlovin, M. M. Glazov, A.V. Sel'kin, and A. V. Koudinov. This work was partially supported by the Russian Ministry of Education and Science (Contract No. 11.G34.31.0067 with SPbSU). The authors acknowledge Saint Petersburg State University for Research Grant No. 11.38.213.2014.

APPENDIX A

According to Eqs. (10) and (11), the uniaxial stress gives rise to k -linear terms in the Hamiltonians of both electrons and holes. As a consequence, the terms that are linearly dependent on the wave vector K appear in the exciton Hamiltonian. To find these terms, one should go from operators \hat{k}_α to the operators \hat{K} and \hat{p}_α by means of substitution of expressions (1) in Eqs. (10) and (11). This substitution gives rise to many terms in the exciton Hamiltonian. We consider only the terms linearly dependent on \hat{K}_z . Other terms contain operators $\hat{p}_x, \hat{p}_y, \hat{p}_z$, which mix $1s$ - and np -excitonic states and lead to a shift of the excitonic spectrum as a whole. Since this shift is much less than the shift of the excitonic spectrum described by the Bir-Pikus Hamiltonian (9), we ignore it in the further analysis.

Among the terms linearly dependent on \hat{k}_z , the first and the last terms in Eq. (11) can be excluded from consideration because \hat{k}_z is present only in terms containing J_x, J_y , and

V_z . These terms describe the mixing of the light-hole and heavy-hole excitons, whose strength is inversely proportional to the splitting of these excitons described by H_ε [see Eq. (9)]. For the characteristic magnitudes of the exciton wave vector K considered in our work, $H_\varepsilon \gg H_v^{(ek)}$, therefore such mixing has little effect on the energy of exciton, and we neglect it. We also do not consider the operator described by Eq. (10), since constants C_3 and C'_3 are much less than C_6 and C_8 entering Eq. (11).

Besides the above terms, there are k -linear contributions to the hole Hamiltonian which are independent of strain [24]. These terms mix states of the heavy and light holes, as well as the ground and excited states of the exciton. Our analysis shows that they do not result in k -linear splitting of $1s$ -exciton states. Material constants determining the magnitude of the mixing are small for most crystals, therefore these terms are not considered in the present work.

APPENDIX B

The electric-field amplitudes, E_i, E_{ri}, E_x , and E_p , are related to each other by the Maxwell's and Pekar's boundary conditions:

$$\begin{aligned} E_i + E_{ri} &= E_x + E_p, \\ n_0 E_i - n_0 E_{ri} &= n_{x+} E_x + n_{p+} E_p, \\ \chi(K_{x+}, \omega) E_x + \chi(K_{p+}, \omega) E_p &= 0, \end{aligned} \quad (\text{B1})$$

where

$$\chi(K_{p,x+}) = \frac{\epsilon_0 \hbar^2 \omega_{LT}}{H_{Xh} + H_{eh} + A_{3/2} K_{p,x\pm}}.$$

From these conditions, we find the amplitude coefficients for transmission and reflection:

$$\begin{aligned} r_{00} &= \frac{E_{ri}}{E_i} = \frac{-n_{p+} + \alpha_+^+ n_{x+} + (1 - \alpha_+^+) n_0}{n_{p+} - \alpha_+^+ n_{x+} + (1 - \alpha_+^+) n_0}, \\ t_{0p}^+ &= \frac{E_p}{E_i} = \frac{2n_0}{n_{p+} - \alpha_+^+ n_{x+} + (1 - \alpha_+^+) n_0}, \\ t_{0x}^+ &= \frac{E_x}{E_i} = \frac{-2\alpha_+^+ n_0}{n_{p+} - \alpha_+^+ n_{x+} + (1 - \alpha_+^+) n_0}, \end{aligned} \quad (\text{B2})$$

where

$$\alpha_+^+ = \frac{\chi(K_{p+}, \omega)}{\chi(K_{x+}, \omega)}.$$

Here, to simplify the notation of coefficients, the plus and minus signs indicating the direction of the wave propagation are transferred from the subscripts to the superscripts.

[1] G. Dresselhaus, *Phys. Rev.* **100**, 580 (1955).

[2] Yu. L. Bychkov and E. I. Rashba, *J. Phys. C* **17**, 6039 (1984).

[3] P. S. Eldridge, W. J. H. Leyland, P. G. Lagoudakis, R. T. Harley, R. T. Phillips, R. Winkler, M. Henini, and D. Taylor, *Phys. Rev. B* **82**, 045317 (2010).

[4] S. D. Ganichev and L. E. Golub, [arXiv:1310.4089](https://arxiv.org/abs/1310.4089)

[5] D. J. English, P. G. Lagoudakis, R. T. Harley, P. S. Eldridge, J. Hubner, and M. Oestreich, *Phys. Rev. B* **84**, 155323 (2011).

[6] W. Knap, C. Skierbiszewski, A. Zduniak, E. Litwin-Staszewska, D. Bertho, F. Kobbi, J. L. Robert, G. E. Pikus, F. G. Pikus, S. V. Iordanskii, V. Mosser, K. Zekentes, and Yu. B. Lyanda-Geller, *Phys. Rev. B* **53**, 3912 (1996).

- [7] J. B. Miller, D. M. Zumbuhl, C. M. Marcus, Y. B. Lyanda-Geller, D. Goldhaber-Gordon, K. Campman, and A. C. Gossard, *Phys. Rev. Lett.* **90**, 076807 (2003).
- [8] M. M. Glazov and L. E. Golub, *Semicond. Sci. Technol.* **24**, 064007 (2009).
- [9] S. D. Ganichev, V. V. Bel'kov, Petra Schneider, E. L. Ivchenko, S. A. Tarasenko, W. Wegscheider, D. Weiss, D. Schuh, E. V. Berezulin, and W. Prettl, *Phys. Rev. B* **68**, 035319 (2003).
- [10] E. L. Ivchenko and A. V. Selkin, *Zh. Eksp. Teor. Fiz.* **76**, 1837 (1979) [*JETP* **49**, 933 (1979)].
- [11] L. E. Golub, *Europhys. Lett.* **98**, 54005 (2012).
- [12] V. P. Mineev and Yu. Yoshioka, *Phys. Rev. B* **81**, 094525 (2010).
- [13] P. Hosur, A. Kapitulnik, S. A. Kivelson, J. Orenstein, and S. Raghu, *Phys. Rev. B* **87**, 115116 (2013).
- [14] K. S. Novoselov, A. K. Geim, S. V. Morozov, D. Jiang, Y. Zhang, S. V. Dubonos, I. V. Grigorieva, and A. A. Firsov, *Science* **306**, 666 (2004).
- [15] Xiao-Liang Qi and Shou-Cheng Zhang, *Rev. Mod. Phys.* **83**, 1057 (2011).
- [16] K. S. Novoselov, A. K. Geim, S. V. Morozov, D. Jiang, M. I. Katsnelson, I. V. Grigorieva, S. V. Dubonos, and A. A. Firsov, *Nature (London)* **438**, 197 (2005).
- [17] M. Muhlbauer, A. Budewitz, B. Buttner, G. Tkachov, E. M. Hankiewicz, C. Brune, H. Buhmann, and L. W. Molenkamp, *Phys. Rev. Lett.* **112**, 146803 (2014).
- [18] A. V. Kavokin, M. Vladimirova, B. Jouault, T. C. H. Liew, J. R. Leonard, and L. V. Butov, *Phys. Rev. B* **88**, 195309 (2013).
- [19] H. Sigurdsson, T. C. H. Liew, O. Kyriienko, and I. A. Shelykh, *Phys. Rev. B* **89**, 035302 (2014).
- [20] A. Tredicucci, Y. Chen, F. Bassani, J. Massies, C. Deparis, and G. Neu, *Phys. Rev. B* **47**, 10348 (1993).
- [21] J. J. Davies, D. Wolverson, V. P. Kochereshko, A. V. Platonov, R. T. Cox, J. Cibert, H. Mariette, C. Bodin, C. Gourgon, I. V. Ignatiev, E. V. Ubylvovk, Y. P. Efimov, and S. A. Eliseev, *Phys. Rev. Lett.* **97**, 187403 (2006).
- [22] S. A. Markov, R. P. Seisyan, and V. A. Kosobukin, *Fiz. Tekh. Poluprovodn. (St. Petersburg)* **38**, 230 (2004) [*Semiconductors* **38**, 225 (2004)].
- [23] D. K. Loginov, E. V. Ubyivovk, Yu. P. Efimov, V. V. Petrov, S. A. Eliseev, Yu. K. Dolgikh, I. V. Ignat'ev, V. P. Kochereshko, and A. V. Sel'kin, *Fiz. Tverd. Tela (St. Petersburg)* **48**, 1979 (2006) [*Phys. Solid State* **48**, 2100 (2006)].
- [24] G. Pikus, V. Maruschak, and A. Titkov, *Fiz. Tekh. Poluprovodn.* **23**, 185 (1988) [*Sov. Phys. Semicond.* **22**, 115 (1988)].
- [25] J. M. Luttinger, *Phys. Rev.* **102**, 1030 (1956).
- [26] Evan O. Kane, *Phys. Rev. B* **11**, 3850 (1975).
- [27] A. Baldereschi and N. C. Lipari, *Phys. Rev. B* **3**, 439 (1971).
- [28] E. L. Ivchenko and G. Pikus, *Superlattices and Other Microstructures* (Springer-Verlag, Berlin, 1995).
- [29] F. H. Pollak and M. Kardona, *Phys. Rev.* **172**, 816 (1968).
- [30] S. I. Pekar, *Zh. Eksperim. I Teor. Fiz.* **33**, 1022 (1957) [*Sov. Phys. JETP* **6**, 785 (1958)].
- [31] Yasuo Nozue, Manabu Itoh and Kikuo Cho, *J. Phys. Soc. Jpn.* **50**, 889 (1981).
- [32] P. Etchegoin, J. Kircher, M. Cardona, C. Grein, and E. Bustarret, *Phys. Rev. B* **46**, 15139 (1992).
- [33] V. M. Agranovich and V. L. Ginzburg, *Crystal Optics with Spatial Dispersion and the Exciton Theory*, 2nd ed. (Springer, New York, 1984).
- [34] M. Born and E. Wolf, *Principles of Optics* (Pergamon, London, 1970).
- [35] L. Schultheis, J. Kuhl, A. Honold, and C. W. Tu, *Phys. Rev. Lett.* **57**, 1797 (1986).
- [36] G. E. Stillman, D. M. Larsen, C. M. Wolfe, and R. C. Brandt, *Solid State Comm.* **9**, 2245 (1971).
- [37] P. Lawaetz *Phys. Rev. B* **4**, 3460 (1971).
- [38] M. S. Skolnickts, A. K. Jaint, R. A. Stradling, J. Leontin, J. C. Ousset, and S. Askenazy, *J. Phys. C* **9**, 2809 (1976).
- [39] M. D. Sturge, *Phys. Rev.* **127**, 768 (1962).
- [40] F. Cerdeira, C. J. Buchenauer, Fred H. Pollak, and Manuel Cordona, *Phys. Rev. B* **5**, 580 (1972).
- [41] D. E. Aspnes and M. Cardona, *Phys. Rev. B* **17**, 741 (1978).
- [42] M. Cardona, *Phys. Status Solidi B* **198**, 5 (1996).